

Nathan A. Crowder · Douglas R. Wylie

Responses of optokinetic neurons in the pretectum and accessory optic system of the pigeon to large-field plaids

Accepted: 2 January 2002 / Published online: 7 February 2002
© Springer-Verlag 2002

Abstract The accessory optic system and pretectum are highly conserved brainstem visual pathways that process the visual consequences of self-motion (i.e. optic flow) and generate the optokinetic response. Neurons in these nuclei have very large receptive fields in the contralateral eye, and exhibit direction-selectivity to large-field moving stimuli. Previous research on visual motion pathways in the geniculostriate system has employed “plaids” composed of two non-parallel sine-wave gratings to investigate the visual system’s ability to detect the global direction of pattern motion as opposed to the direction of motion of the components within the plaids. In this study, using standard extracellular techniques, we recorded the responses of 47 neurons in the nucleus of the basal optic root of the accessory optic system and 49 cells in the pretectal nucleus lentiformis mesencephali of pigeons to large-field gratings and plaids. We found that most neurons were classified as pattern-selective (41–49%) whereas fewer were classified as component-selective (8–17%). There were no striking differences between nucleus of the basal optic root and lentiformis mesencephali neurons in this regard. These data indicate that most of the input to the optokinetic system is orientation-insensitive but a small proportion is orientation-selective. The implications for the connectivity of the motion processing system are discussed.

Keywords Plaids · Optic flow · Aperture problem · Optokinetic nystagmus · Sine-wave gratings

Abbreviations *AOS* accessory optic system · *LM* lentiformis mesencephali · *nBOR* nucleus of the basal optic root · *OKN* optokinetic nystagmus · *SF* spatial

frequency · *TF* temporal frequency · *V1* primary visual cortex

Introduction

Neurons in the accessory optic system (AOS) and pretectum are important for the analysis of the optic flow that results from self-motion (Gibson 1954), and the generation of optokinetic nystagmus (OKN) to facilitate gaze stabilization. AOS and pretectal neurons exhibit direction-selectivity in response to moving large-field stimuli that are rich in visual texture (for reviews see Simpson 1984; Simpson et al. 1988; Grasse and Cyander 1990).

Previous psychophysical and neurophysiological studies of motion sensitive pathways within the geniculostriate system, which is more concerned with object-motion as opposed to self-motion (Frost 1982, 1985; Frost et al. 1990, 1994), have used “plaids” to illustrate the two-stage process of motion perception (motion integration) (Adelson and Movshon 1982; Albright 1984; Movshon et al. 1985; Rodman and Albright 1989; Welch 1989; Gizzi et al. 1990; Scannell et al. 1996; Merabet et al. 1998). The features of a sine-wave grating allow only one dimension of movement to be visible; therefore any motion detected is indistinguishable from motion perpendicular to the orientation of the grating. For plaids composed of symmetrically moving gratings (so-called “type I” plaids; Ferrera and Wilson 1990) the perceived movement appears as a velocity vector that bisects the angle separating the orientation of its component gratings, even though no local motion components are moving in that direction (e.g., Adelson and Movshon 1982; Welch 1989; Stoner and Albright 1992). Most directionally selective neurons in the primary visual cortex (V1) respond to the individual components within a plaid (“component-selective neurons”) indicating that the motion detectors in V1 are orientation-sensitive (Movshon et al. 1985; Gizzi et al. 1990). Neurons in extrastriate areas respond to the global

N.A. Crowder · D. R. Wylie (✉)
Department of Psychology, Center for Neuroscience,
University of Alberta, Edmonton, Alberta, Canada T6G 2E1
E-mail: dwylie@ualberta.ca
Tel.: +1-780-4925274
Fax: +1-780-4921768

direction of motion, reflecting an integration of many orientation-sensitive motion direction signals into a global motion direction (“pattern-selective neurons”; Albright 1984; Rodman and Albright 1989; Gizzi et al. 1990; Stoner and Albright 1992; Scannell et al. 1996). Motion sensitive neurons that have orientation-insensitive inputs would also be expected to respond as pattern-selective neurons (see Smith and Harris 1991).

Smith and Harris (1991) recorded the OKN in cats in response to plaid stimuli. The eye movements were predominantly in the direction of the components of the plaid, (although always biased toward the direction of the overall pattern). Based on the implicit assumption that the retinal input calculates overall direction of motion “directly” (i.e., the retinal input is orientation-insensitive), Smith and Harris (1991) concluded that the OKN in cats is primarily driven by cortical component-selective neurons. In cats there is a rather robust projection from visual cortical areas to the AOS and pretectum (Schoppmann 1981; see also Grasse and Cynader 1990).

In the present study we recorded the responses of optokinetic neurons in the pigeon’s visual system to large-field gratings and plaids. In birds, OKN is mediated by the pretectal nucleus lentiformis mesencephali (LM) and the nucleus of the basal optic root (nBOR) of the AOS (Fite et al. 1979; McKenna and Wallman 1985; Gioanni et al. 1983a, 1983b). The LM and nBOR are retinal recipient (Karten et al. 1977; Reiner et al. 1979; Fite et al. 1981; Gamlin and Cohen 1988a) and also receive input from the visual wulst (the homolog of mammalian visual cortex; Karten and Shimizu 1989) although this projection is sparse (Miceli et al. 1979; Azevedo et al. 1983; Rio et al. 1983). Given the sparse cortical projection, one might expect that the LM and nBOR neurons would show pattern-selective as opposed to component-selective responses.

Materials and methods

Surgery and extracellular recording

Silver King and Racing Homer pigeons were anesthetized with an intramuscular injection of a ketamine (65 mg kg⁻¹)/xylazine (8 mg kg⁻¹) cocktail; supplemental doses were administered as necessary. Animals were placed in a stereotaxic device with pigeon ear bars and beak adapter such that the orientation of the skull conformed to the atlas of Karten and Hodos (1967). Based on the stereotaxic coordinates of Karten and Hodos (1967), sections of bone and dura were removed to expose the brain and allow access to either nBOR or LM.

Extracellular recordings were made with either tungsten microelectrodes (2–5 MΩ impedance; Frederick Haer) or glass micropipettes (4–5 μm tip diameter, containing 2 mol l⁻¹ NaCl), which were lowered into nBOR or LM with a hydraulic microdrive (Frederick Haer). The signal was amplified, filtered, fed through a window discriminator, and displayed on an oscilloscope. The window discriminator produced TTL pulses, each representing single spikes, which were fed into a 1401plus (Cambridge Electronic Designs; CED). The stimuli (see below) were synchronized with the collection of TTL pulses, and peristimulus time histograms were constructed with Spike2 for Windows software (CED).

Stimulus presentation

After neurons in either nBOR or LM were isolated, the optic flow preference and approximate receptive field location of the neuron was determined by moving a large (90°×90°) hand-held stimulus in various directions in the contralateral visual field. Once the receptive field of a neuron was established, the responses to sine-wave gratings and plaids were obtained. These stimuli were generated by a VSGThree graphics computer (Cambridge Research Services), and were displayed in one of two ways: either a SONY multiscan 17se II computer monitor or a data projector (*InFocus* LP750) that back-projected the images onto a tangent screen. For the monitor, the diameter of the stimulus measured 35° visual angle, and for the back-projected stimulus the diameter was 75°.

Initially, the cell was presented with gratings of varying spatial and temporal frequencies [SF, 0.03–2 cycles per degree (cpd); TF, 0.03–16 Hz]. Sine-wave gratings are very effective stimuli for AOS and pretectal neurons (Ibbotson et al. 1994; Wolf-Oberhollenzer and Kirschfeld 1994; Wylie and Crowder 2000; Crowder and Wylie 2001). The stimulus was oscillated along the preferred axis to determine the optimal spatial (SF) and temporal frequencies (TF), although nBOR and LM neurons are broadly tuned in this respect (see Wylie and Crowder 2000; Crowder and Wylie 2001). Direction-tuning curves (response as a function of the direction of motion) were then established. Each neuron was tested with gratings and 135° plaids (i.e., symmetrical plaids with component gratings separated by 135°) in 16 directions, and/or gratings and 150° plaids in 24 directions. The gratings used for the directional tuning were of an optimal SF and TF. The SF for the plaids was of the same SF used for the gratings. The TF of the plaids was adjusted such that the overall pattern velocity matched that of the gratings. Each sweep consisted of a 4-s motion in one direction, a 3-s pause, a 4-s motion in the opposite direction, followed by a 3-s pause. For single gratings, the contrast was 0.95 [where the conventional definition of contrast was used; (Luminance_{MAX}–Luminance_{MIN})/(Luminance_{MAX} + Luminance_{MIN})]. The plaids were generated by simultaneously displaying two non-parallel sine-wave gratings of half the contrast of the grating stimuli. Thus, the overall contrast of the plaids was also 0.95. During the pause the stimulus was a uniform gray of the standard mean luminance. Within a block of trials, the presentation of gratings, plaids, and directions was randomized to reduce the effect of response variability. The resultant directional tuning curves in response to plaids and gratings were averaged over 3–8 sweeps.

Data analysis

The direction tuning curves in response to the gratings were then used to generate the predicted pattern and component responses to the plaids. The procedure for distinguishing between such component and pattern selective neurons is illustrated in Fig. 1. Polar plots of the idealized directional tuning curves in response to single gratings and plaids are shown for pattern-selective and component-selective neurons. A pattern-selective neuron shows identical directional tuning to gratings and plaids (Fig. 1, left side), while the tuning curve for the predicted component response was calculated, from the tuning curve in response to gratings, by taking the sum of the two components of the plaid for each direction (Fig. 1, right side). Following Movshon et al. (1985) cells were classified as component or pattern selective by comparing the direction tuning curves for the plaids to the predicted component response and the predicted pattern response using the following formula:

$$R_P = (r_P - r_C * r_{PC}) / [(1 - r_C^2) * (1 - r_{PC}^2)]^{1/2} \quad (1)$$

where, R_P is the partial correlation coefficient for the pattern prediction, r_C is the correlation coefficient of the plaid response with the component prediction, r_P is the correlation coefficient of the plaid response with the pattern prediction, and r_{PC} is the correlation coefficient of the of the pattern and component predictions.

Predictions

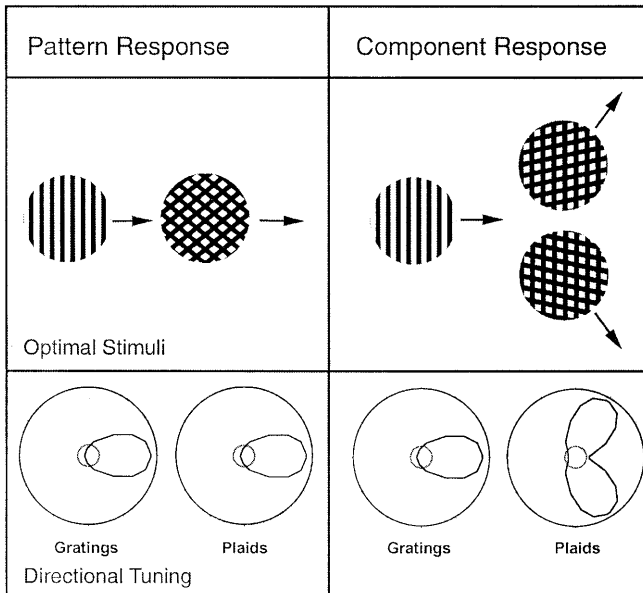


Fig. 1. Idealized pattern (*left*) and component (*right*) responses for directionally selective neurons. For hypothetical neurons that prefer rightward motion, the responses to single gratings, and plaids composed of two overlapping gratings separated by 120° (120° plaids). On the left, the optimal stimuli (*top*) and directional tuning curves (*bottom*) for gratings and plaids are shown for a pattern-selective neuron. Direction tuning is plotted in polar coordinates where the radius represents neuronal response magnitude, and polar angle represents the direction of the stimulus motion. The plaid tuning curve is identical to that of the single grating, indicating sensitivity of the neuron to the direction of coherent pattern motion and not the individual components within the plaid. On the right, the optimal stimuli (*top*) and directional tuning curves (*bottom*) for gratings and plaids are shown for a component-selective neuron. The response to a plaid in a given direction is the sum of the response to the two components. Thus, the optimal plaid stimuli contain a component that is moving rightward and the overall tuning curve reflects the sensitivity to directions of both components within the plaid. Adapted from Rodman and Albright (1989)

To calculate the partial correlation coefficient for the component motion prediction (R_C), r_P is exchanged with r_C and visa versa.

The statistical significance of R_P and R_C was calculated by performing a Fisher Z-transform on the correlation coefficients $\{Zf = 1/2 \times \ln[(1+R)/(1-R)]\}$, and then calculating the difference between these z-scores (Papoulis 1990):

$$z = (Zf_P - Zf_C) / (1/N_P - 3 + 1/(N_C - 3))^{1/2} \quad (2)$$

where Zf_P is the Fisher Z-transform for R_P , Zf_C is the Fisher Z-transform for R_C , $N_P = N_C =$ number of directions (16 for 135° plaids, or 24 for 150° plaids).

These data were then plotted as in Fig. 2 (adapted from Movshon et al. 1985; Gizzi et al. 1990; Scannell et al. 1996). The abscissa plots the component-prediction correlations (R_C) and the ordinate plots the pattern-prediction correlations (R_P). The scatter plot is divided into three regions, which are marked by solid lines for 150° plaids and dashed lines for 135° plaids. The region marked "Component Cells" contains those cells for which the component prediction significantly exceeds either zero or the value of the pattern prediction. Similarly, the region marked "Pattern Cells" contains those cells for which the pattern prediction significantly exceeds either zero or the value of the component pre-

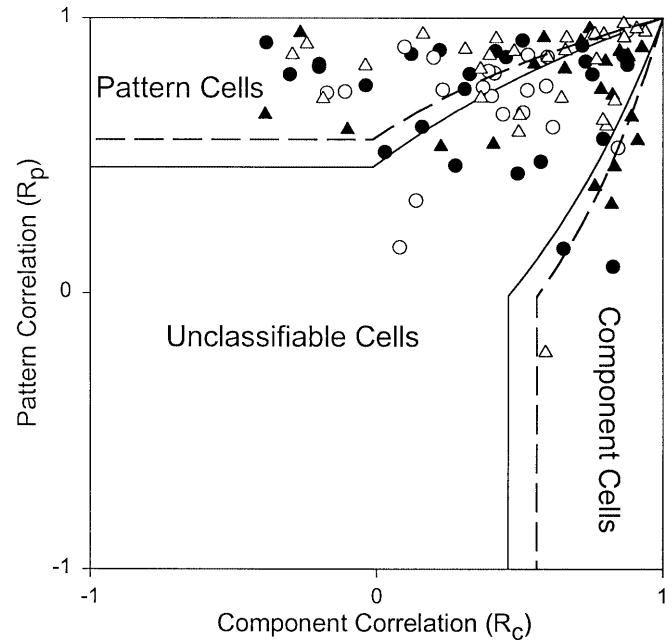


Fig. 2. Scatter plots of partial correlations for pattern (R_P) and component (R_C) selectivity. Each data point indicates the degree to which the direction tuning for nucleus of the basal optic root (nBOR) and lentiformis mesencephali (LM) neurons are correlated with pattern and component predictions. The data space is divided into three regions based on statistical criteria by a solid line for 150° plaids and a dashed line for 135° plaids (see Materials and methods). Cells falling in the upper left, middle, or lower right areas are classified as pattern selective, unclassifiable, or component selective, respectively. The nBOR neurons are shown as filled circles (150° plaids) or triangles (135° plaids), and the LM neurons are shown as empty circles (150° plaids) or triangles (135° plaids). Note the predominance of pattern-selective neurons

diction. The region marked "Unclassifiable Cells" contains cells where the two predictions do not significantly differ from each other or from zero. The conventional criterion probability of 0.1 was used to define the three regions in the scatter plot (Crow et al. 1960). This criterion has been justified by the fact that this method is not a true test for statistical significance, but a convenient way to reduce data (Movshon et al. 1985; Gizzi et al. 1990; Scannell et al. 1996). Clearly, neurons whose firing properties are better described by the component prediction will fall in the "Component" region, and neurons whose firing properties are better described by the pattern prediction will fall in the "Pattern" region. Neurons may fall in the "Unclassifiable" region because their data is too variable to permit satisfactory analysis, or because the two predictions are too similar to be distinguished by the partial correlation computation.

There are other problems associated with using this statistical method for classification. For example, this partial correlation method effectively compares the shape of the tuning curves but does not take into account absolute depth of modulation. Thus, we also classified the neurons as pattern-selective, component-selective, or unclassifiable by visual inspection of the tuning curves.

Histology

In some cases, when the tungsten microelectrodes were used, electrolytic lesions (30 μA , 10 s, electrode +ve) were made at known locations relative to recording sites. At the end of the experiment, animals were given a lethal dose of sodium pentobarbital (100 mg kg^{-1} i.p.) and immediately perfused with saline followed by 4% para-formaldehyde. The brains were extracted, post-fixed for several hours (4% para-formaldehyde with 20% sucrose) and then left in 30% sucrose for at least 24 h. Using a microtome, frozen sections (45 μm thick in the coronal plane) through the brainstem and pretectum were collected. The sections were mounted onto gelatin coated slides, dried, counterstained with neutral red, and coverslipped with Permount. Light microscopy was used to localize electrode tracts and the lesion sites.

Results

Quantitative data was obtained from 47 nBOR neurons and 49 LM neurons (from 38 birds). LM and nBOR neurons have large receptive fields (30–150° diameter) in the contralateral eye, and exhibit directional tuning in response to moving largfield stimuli. Most neurons are spontaneously active and motion in one direction (the “preferred” direction) results in excitation, whereas motion in the opposite direction results in inhibition (the “anti-preferred” direction). These properties have been examined extensively elsewhere and will not be discussed (Burns and Wallman 1981; Morgan and Frost 1981; Winterson and Brauth 1985; Wylie and Frost 1990; Wylie and Crowder 2000; for reviews see Simpson 1984; Simpson et al. 1988; Grasse and Cynader 1990).

As described in Materials and methods, directional tuning curves in response to plaid stimuli were compared to pattern-selective and component-selective predictions, and partial correlations (R_p and R_c) were calculated.

Figure 2 shows the distribution of nBOR neurons as filled circles (150° plaids) or triangles (135° plaids), and the distribution of LM neurons as empty circles (150° plaids) or triangles (135° plaids); the predominance of pattern-selectivity is evident. Of the 47 direction selective units recorded from nBOR, 21 (45%) cells were classified as pattern cells, 6 (13%) cells were classified as component cells, and the remaining 20 (43%) cells fell in the unclassifiable region. Of the 49 direction-selective units recorded from LM, 26 (53%) cells were classified as pattern cells, 2 (4%) were classified as component cells, and 21 (43%) cells fell in the unclassifiable region. Collapsing the LM and nBOR samples, of 96 cells, 47 (49%) were pattern-selective, 8 (8%) were component-selective, and 41 (43%) were unclassifiable.

In Fig. 3, direction-tuning curves of representative LM (Fig. 3a–d) and nBOR (Fig. 3e–h) neurons that were selective for pattern motion are shown. In this and subsequent figures, the firing rate relative to the spontaneous rate is plotted as a function of the direction of motion in polar coordinates (polar plots). Directional tuning curves of the predicted component-selective responses to plaids, and the neuronal responses to gratings and plaids are shown as dashed, dotted, and solid lines,

respectively. Error bars, representing ± 1 standard deviation (SD), are shown for the cell in Fig. 3a. The values of R_p and R_c , as well as the type of plaid used, is also indicated for each neuron. The close correspondence between tuning curves in response to gratings and in response to plaids indicates that these neurons signal the global direction of motion irrespective of local motion signals. In some cases, for example the neuron in Fig. 3c, there is clearly a very tight correspondence between the response to plaids and the response to gratings. In Fig. 3g, note that the two small lobes on the plaid tuning curve in response to upward and downward motion are in the direction of the two maxima of the predicted component response. For the cells in Fig. 3e, f, the response to the plaids was actually greater than the response to gratings, although this was uncommon.

Figure 4 shows polar plots of direction tuning curves representative of nBOR (Fig. 4a, b, d) and LM (Fig. 4c) neurons selective for component motion. For these neurons, the tuning curves in response to plaids closely correspond to the predicted tuning curves for component-selective responses. The cell shown in Fig. 4c was one of two LM cells that were classified as component selective based on statistical criteria. This cell was somewhat odd: whereas all other LM cells we recorded from showed a unidirectional tuning curve in response to gratings, this had a bi-directional response to gratings. That is, gratings moving forward and backward resulted in an approximately equal amount of excitation. Such bi-directional LM cells have been reported previously (Wylie and Crowder 2000). In response to plaids, the neuron was excited by upward and downward motion, matching the component prediction.

Figure 5 shows tuning curves of other nBOR (Fig. 5b, f, g, h) and LM (Fig. 5a, c, d, e) neurons that could not be classified as pattern- or component-selective. A number of neurons were unclassifiable because they showed an attenuated response to plaids (Fig. 5a–c, f), and some neurons did not respond at all to the plaids (Fig. 5d). For the neurons shown in Fig. 5c, g, h the pattern and component predictions are quite similar, which reduces the likelihood of finding a definitive difference between the two predictions (Stoner and Albright 1994). For the neurons in Fig. 5e–h the directional tuning curve in response to plaids falls somewhere between those of the component-selective and pattern-selective predictions.

Classification by visual inspection

We also classified cells as pattern-selective, component-selective or unclassifiable based on a simple visual inspection of the tuning curves. Using this subjective method, of the 47 nBOR cells, 17 (36%) cells were classified as pattern cells, 9 (19%) cells were classified as component cells, and the remaining 21 (45%) cells fell in the unclassifiable region. Of the 49 LM neurons, 22 (45%) cells were classified as pattern cells, 7 (14%) were

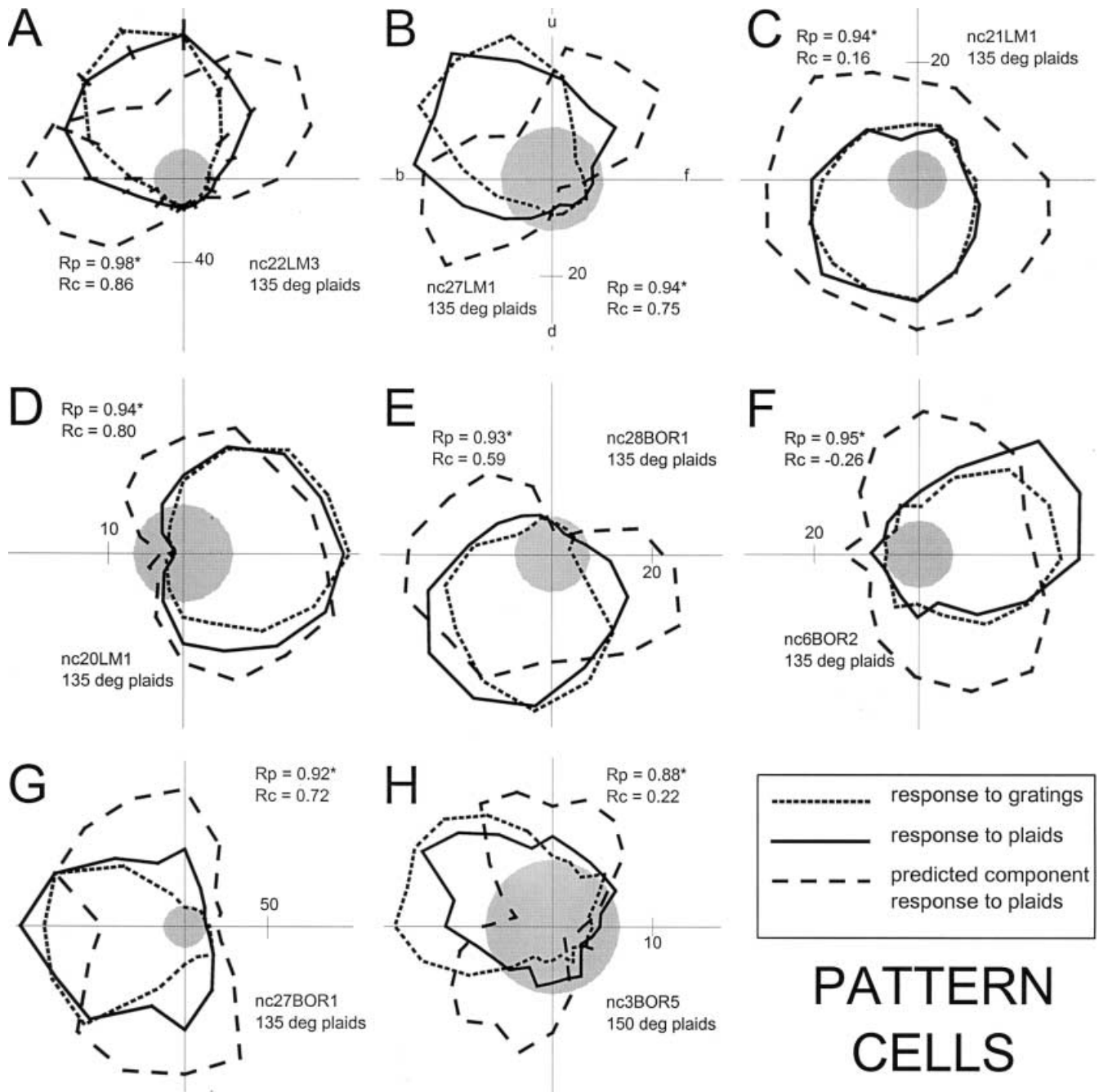


Fig. 3. Polar plots illustrating the responses (spikes s^{-1}) of pattern-selective LM (a–d) and nBOR (e–h) neurons to gratings and plaids. Firing rate relative to the spontaneous rate (SR ; gray circle) is plotted as a function of the direction of motion in polar coordinates. (i.e., the SR has been set to zero; outside the gray circle = excitation, inside = inhibition). The responses to gratings and plaids are shown as dotted and solid lines, respectively. The predicted response to plaids for component-selective neurons is shown with a dashed line (see Fig. 1, and Materials and methods). Error bars representing ± 1 standard deviation (SD) are shown for the neuron in a. u , b , d , and f represent up, back (nasal to temporal), down, and forward (temporal to nasal) motion, respectively. Partial correlations (R_p and R_c) for each neuron are also shown; an asterisk indicates statistical significance ($P < 0.1$). The type of plaid (135° or 150°) used is also indicated.

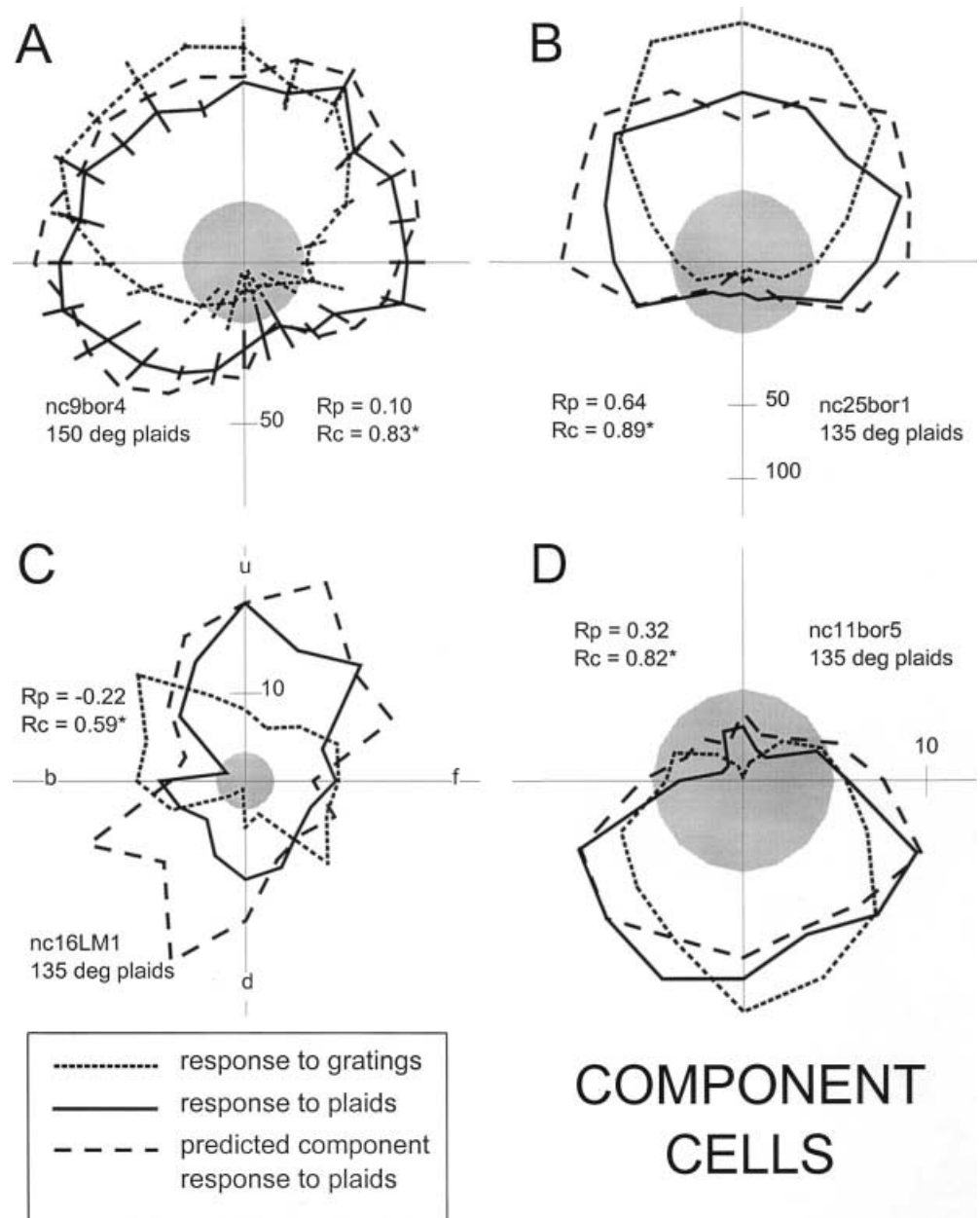
classified as component cells, and 20 (41%) cells fell in the unclassifiable region. Collapsing the LM and nBOR samples, of 96 cells, 39 (41%) were pattern selective, 16 (17%) were component selective, and 41 (43%) were unclassifiable. Thus, compared with the partial correlation analysis, the inspection method results in slightly fewer pattern-selective neurons (41% versus 48%) and doubles the proportion of neurons classified as component selective (17% versus 8%). Comparing the two methods of classification for individual cells, there was a concordance rate of 81% (78/96). Of the discordances, there were 8 cells classified as pattern selective with the statistical method that were unclassifiable by inspection.

Two cells, unclassifiable by the statistical method were pattern selective by inspection. Two cells were pattern-selective with the statistical method, but component-selective by inspection. Finally, there were 6 cells that were unclassifiable by the partial correlation method that were appeared to be component selective by inspection. Four of these cells are shown in Fig. 6, in addition to a cell that was pattern-selective based on the statistical criteria but component-selective by inspection. For all of these cells, it appeared that the tuning curve in response to plaids resembles the predicted component response as opposed to the predicted pattern response. This is particularly evident for Fig. 6b For some of these cells, R_C was greater than R_P , although the difference was not significant (e.g., Fig. 6a, b).

Discussion

In the present study, following the methods of previous studies of direction selective neurons in mammalian visual cortex, we recorded the responses of optokinetic neurons to large-field gratings and plaids. Most cells in the nBOR and LM were pattern-selective, about 50% according to the statistical classification proposed by Movshon et al. (1985). Fewer showed component motion selectivity, 13% of the nBOR neurons and 4% of the LM neurons, and many cells were unclassifiable (43%). Stoner and Albright (1994) suggested that this type of classification system should be used with caution. The ability to discriminate pattern- and component-cells

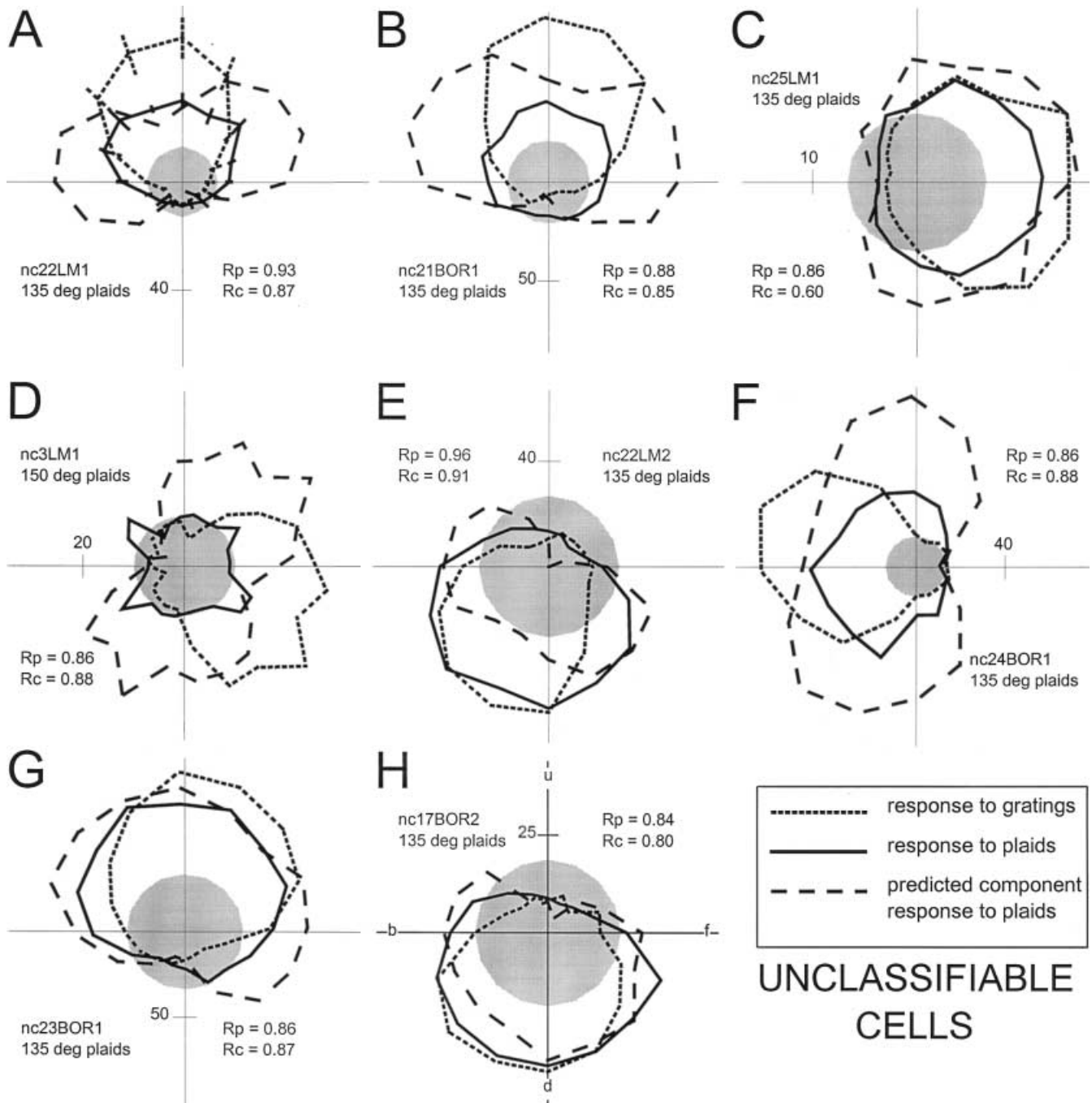
Fig. 4. Polar plots illustrating the responses of component-selective nBOR (a, b, d) and LM (c) neurons to gratings and plaids. See legend to Fig. 3 for details



depends on the similarity between the component and pattern conditions, which is affected by the breadth of directional tuning, and the angular distance between the component and pattern motions. In particular, Stoner and Albright (1994) emphasize that because a neuron is assigned to the unclassifiable group it does not preclude the neuron from being pattern- or component-sensitive. Indeed, with Fig. 6, we assert that several unclassifiable neurons were component by visual inspection.

Fig. 5. Polar plots illustrating the responses of unclassifiable neurons in LM (a, c-e) and nBOR (b, f-h) to gratings and plaids. See legend to Fig. 3 for details. See text for detailed description

Previous studies in the mammalian geniculostriate system have found that most neurons in V1 are component selective, while there are subpopulations of neurons in extrastriate cortex that that are component selective (about 33%), and pattern selective (about 30%; Albright 1984; Movshon et al. 1985; Rodman and Albright 1989; Gizzi et al. 1990; Stoner and Albright 1992; Scannell et al. 1996). This functional separation forms the basis for models where component-selective neurons provide the input for pattern-selective neurons in the cortex (e.g., Movshon et al. 1985; Stoner and Albright 1994), although Merabet et al. (1998) suggested

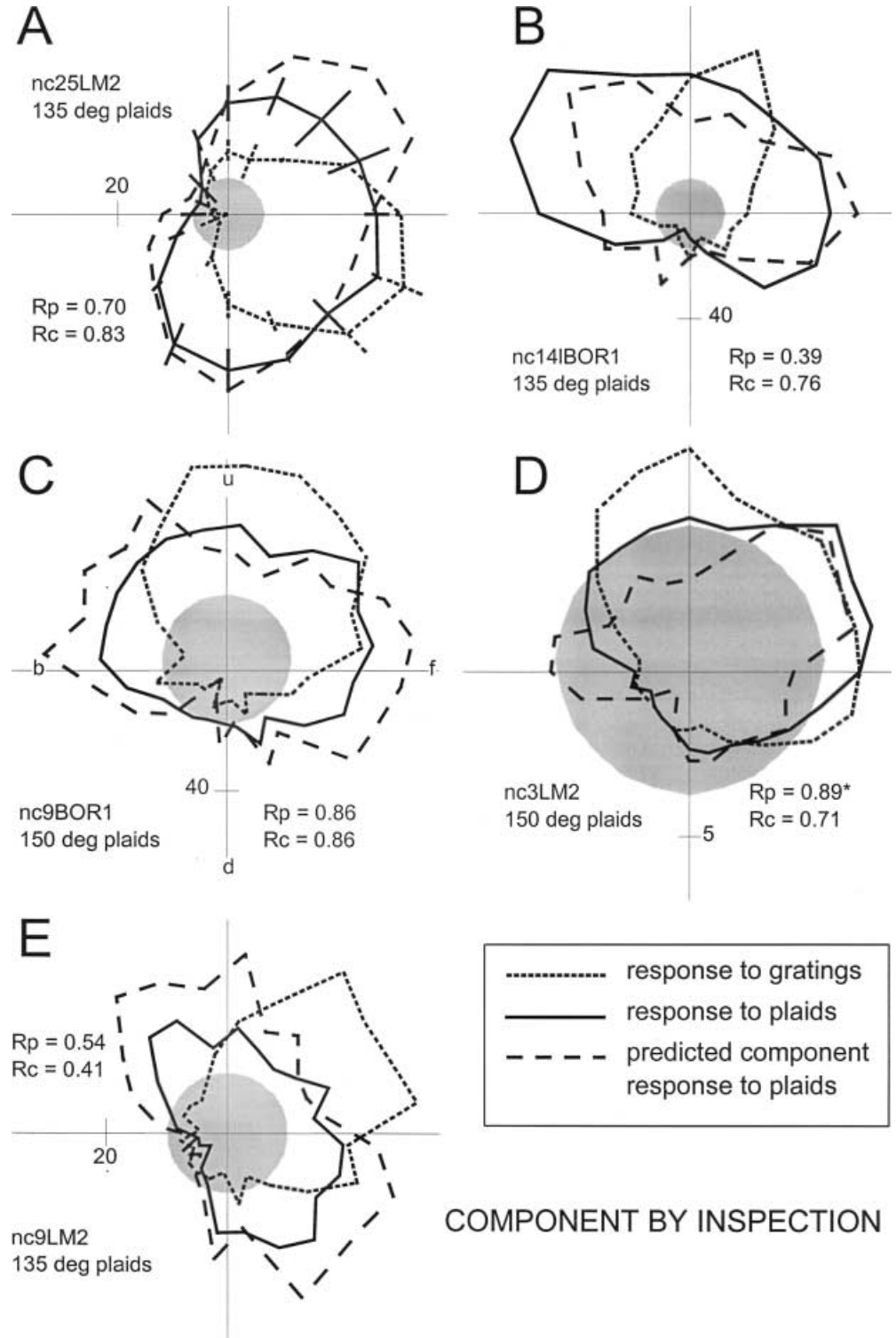


that motion integration results from processing in a number of cortico-thalamic loops.

In the present study we have found that most pre-ectal and AOS neurons exhibit pattern-selectivity. Indeed the percentage of neurons showing pattern-selectivity in the nBOR and LM (~50%) is higher than that reported for studies of extrastriate cortex (~30%;

Albright 1984; Movshon et al. 1985; Rodman and Albright 1989; Stoner and Albright 1992; Scannell et al. 1996). However, this is not to say that this represents motion integration of inputs that are orientation sensitive. It is possible that the pattern motion is detected directly with orientation-insensitive motion detectors (see Smith and Harris 1991).

Fig. 6. Polar plots illustrating the responses of neurons in nBOR (**B, C**) and LM (**A, D, E**) neurons to gratings and plaids. See legend to Fig. 3 for details. For these neurons, although the response to plaids appears to match the predicted component response, these neurons were not classified as component-selective by the statistical criteria



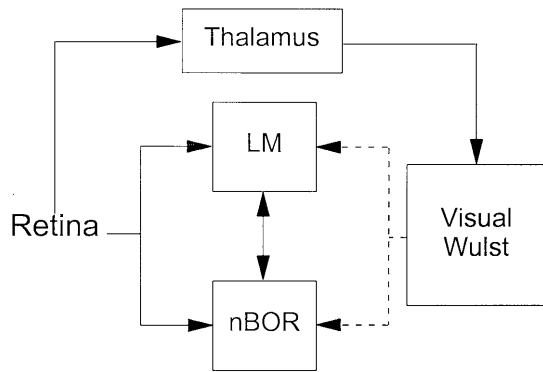


Fig. 7. A simplified schematic of sources of visual information to the nBOR of the accessory optic system, and pretectal nucleus LM. The *dashed lines* represent weaker projections. See text for discussion

Retinal and telencephalic contributions to motion processing in the optokinetic system

In response to large-field plaid stimuli, Smith and Harris (1991) found that in cats, the optokinetic eye movements were predominantly in the direction of the components of the plaid, although always biased in the direction of the overall pattern. They proposed that the motion detectors within the optokinetic system are dominated by descending orientation-sensitive cortical inputs, whereas orientation-insensitive retinal inputs play less of a role.

Given that we found that a majority of AOS and pretectal neurons showed pattern-selectivity, whereas relatively few showed component selectivity, our findings are seemingly at odds with those of Smith and Harris (1991). However, to reiterate, Smith and Harris (1991) suggest that the component-sensitivity in the optokinetic system is due to descending orientation-selective cortical inputs. In pigeons, the descending telencephalic input to the LM and nBOR is considered sparse. Figure 7 shows a schematic of the visual inputs to the optokinetic nuclei in birds. There is a direct retinal input to LM (Gamlin and Cohen 1988a) and nBOR (Karten et al. 1977; Reiner et al. 1979; Fite et al. 1981) in addition to a weaker input from the visual wulst (Karten et al. 1977; Reiner et al. 1979; Fite et al. 1981). (The visual wulst is thought to be the avian homolog of primary visual cortex (Karten and Shimizu 1989). There is also a strong reciprocal connection between LM and nBOR (Clark 1977; Brecha et al. 1980; Gamlin and Cohen 1988b; Wylie et al. 1997). This pattern of connectivity is essentially identical to that found in mammals (see Simpson 1984) except that the cortical input is quite variable between species. The cortical input to the mammalian nucleus of the optic tract (homologous to the avian LM) is quite heavy in cats and monkeys (Schoppmann 1981; Hoffmann et al. 1991; Ilg and Hoffmann 1993; Mustari et al. 1994) but is absent in other frontal-eyed species (opossum; Pereira et al. 2000). A cortical input has also been found in rats (Shintani

et al. 1999), guinea pigs (Lui et al. 1994) and rabbits (Hollander et al. 1979), but not in hamsters (Lent 1982) or tree shrews (Huerta et al. 1985). In animals with a sparse cortical input to the AOS and pretectum there is a strong naso-temporal asymmetry in the OKN (Collewijn 1969; pigeons, Gianni 1988; Zolotilina et al. 1995), which is not apparent in animals with a robust cortical input (e.g., Grasse and Cynader 1990).

The predominance of pattern-selective neurons in LM and nBOR might reflect a large contribution from orientation-insensitive retinal inputs. However, the presence of component-selective cells in the LM and nBOR clearly indicates that orientation-sensitive information is entering the pigeon optokinetic system, perhaps from the visual wulst. Orientation-sensitivity has been demonstrated in the avian wulst (Wilson 1980). Moreover, some of the tuning curves of some pattern-selective (e.g., Fig. 3g) and unclassifiable neurons (e.g., Fig. 6e–h) might represent integration of orientation-insensitive retinal inputs and component-sensitive telencephalic inputs.

As a cautionary note, the assumption that the retinal input is orientation-insensitive has yet to be directly evaluated. Although Smith and Harris (1991) cite the fact that retinal ganglion cells in mammals have circular receptive fields and are orientation insensitive, the AOS and pretectum receive input from a particular class of ganglion cells. In birds, the retinal input to the AOS is only from the displaced ganglion cells (Karten et al. 1977; Reiner et al. 1979; Fite et al. 1981), and we are unaware of any studies addressing their orientation sensitivity. Thus, it is possible that the pattern-selectivity arises from motion integration of retinal inputs, or integration of endogenous connections within and between LM and nBOR. It is also possible that there is integration of descending inputs from the wulst.

Acknowledgements This research was supported by grant funding from the Natural Sciences and Engineering Research Council (NSERC) of Canada to D.R.W. Wylie. N.A. Crowder was supported by summer studentship funding from Alberta Heritage Foundation for Medical Research (AHFMR), and NSERC post-graduate scholarship. We thank W.F. Bischof, J.A. Movshon, and C. Varnhagen for advise on the experimental design and statistical analysis. The methods reported herein conform to the guidelines established by the Canadian Council on Animal Care and were approved by the Biological Sciences Animal Services at the University of Alberta.

References

- Adelson EH, Movshon JA (1982) Phenomenal coherence of moving visual patterns. *Nature* 300:523–525
- Albright TD (1984) Direction and orientation selectivity of neurons in visual area MT of the macaque. *J Neurophysiol* 52:1106–1130
- Azevedo TA, Cukiert A, Britto LRG (1983) A pretectal projection upon the accessory optic nucleus in the pigeon: an anatomical and electrophysiological study. *Neurosci Lett* 43:13–18
- Brecha N, Karten HJ, Hunt SP (1980) Projections of the nucleus of basal optic root in the pigeon: an autoradiographic and horseradish peroxidase study. *J Comp Neurol* 189:615–670

- Burns S, Wallman J (1981) Relation of single unit properties to the oculomotor function of the nucleus of the basal optic root (AOS) in chickens. *Exp Brain Res* 42:171–180
- Clark PGH (1977) Some visual and other connections to the cerebellum of the pigeon. *J Physiol (Lond)* 243:267–285
- Collewijn H (1969) Optokinetic eye movements in the rabbit: input-output relations. *Vision Res* 9:117–32
- Crow EL, Davis FA, Maxfield MW (1960) *Statistics manual, with examples taken from ordinance development*. Dover, New York
- Crowder NA, Wylie DRW (2001) Fast and slow neurons in the nucleus of the basal optic root in pigeons. *Neurosci Lett* 304:133–136
- Ferrera VP, Wilson HR (1990) Perceived direction of moving two-dimensional pattern. *Vision Res* 30:273–287
- Fite KV, Reiner T, Hunt S (1979) Optokinetic nystagmus and the accessory optic system of pigeon and turtle. *Brain Behav Evol* 16:192–202
- Fite KV, Brecha N, Karten HJ, Hunt SP (1981) Displaced ganglion cells and the accessory optic system of pigeon. *J Comp Neurol* 195:279–88
- Frost BJ (1982) Mechanisms for discriminating object motion from self-induced motion in the pigeon. In: Ingle DJ, Goodale MA, Mansfield JW (eds) *Analysis of visual behavior*. MIT Press, Cambridge, pp 177–196
- Frost BJ (1985) Neural mechanisms for detecting object motion and figure-ground boundaries contrasted with self-motion detecting systems. In: Ingle DJ, Jeannerod M, Lee D (eds) *Brain mechanisms of spatial vision*. Martinus Nijhoff, Dordrecht, pp 415–449
- Frost BJ, Wylie DR, Wang Y-C (1990) The processing of object and self-motion in the tectofugal and accessory optic pathways of birds. *Vision Res* 30:1677–1688
- Frost BJ, Wylie DR, Wang Y-C (1994) The analysis of motion in the visual systems of birds. In: Green P, Davies M (eds) *Perception and motor control in birds*. Springer, Berlin Heidelberg New York, pp 249–266
- Gamlin PDR, Cohen DH (1988a) The retinal projections to the pretectum in the pigeon (*Columba livia*). *J Comp Neurol* 269:1–17
- Gamlin PDR, Cohen DH (1988b) Projections of the retinorecipient pretectal nuclei in the pigeon (*Columba livia*). *J Comp Neurol* 269:18–46
- Gibson JJ (1954) The visual perception of object motion and subjective movement. *Psychol Rev* 61:304–314
- Gioanni H (1988) Stabilizing gaze reflexes in the pigeon (*Columba livia*). I. Horizontal and vertical optokinetic eye (OKN) and head (OCR) reflexes. *Exp Brain Res* 69:567–582
- Gioanni H, Rey J, Villalobos J, Richard D, Dalbera A (1983a) Optokinetic nystagmus in the pigeon (*Columba livia*). II. Role of the pretectal nucleus of the accessory optic system. *Exp Brain Res* 50:237–247
- Gioanni H, Villalobos J, Rey J, Dalbera A (1983b) Optokinetic nystagmus in the pigeon (*Columba livia*). III. Role of the nucleus ectomammillaris (nEM): interactions in the accessory optic system. *Exp Brain Res* 50:248–258
- Gizzi MS, Katz E, Schumer RA, Movshon JA (1990) Selectivity for orientation and direction of motion of single neurons in cat striate and extrastriate visual cortex. *J Neurophysiol* 63:1529–1543
- Grasse KL, Cyander MS (1990) The accessory optic system in frontal-eyed animals. In: Leventhal A (ed) *Vision and visual dysfunction. The neuronal basis of visual function*. McMillan, New York, pp 111–139
- Hoffmann KP, Distler C, Erickson RG (1991) Functional projections from striate cortex and superior temporal sulcus to the nucleus of the optic tract (NOT) and dorsal terminal nucleus of the accessory optic tract (DTN) of macaque monkeys. *J Comp Neurol* 313:707–724
- Hollander H, Tietze J, Distel H (1979) An autoradiographic study of the subcortical projections of the rabbit striate cortex in the adult and during postnatal development. *J Comp Neurol* 184:783–794
- Huerta MF, Weber JT, Rothstein LR, Harting JK (1985) Subcortical connections of area 17 in the tree shrew: an autoradiographic analysis. *Brain Res* 340:163–170
- Ibbotson MR, Mark RF, Maddess TL (1994) Spatiotemporal response properties of direction-selective neurons in the nucleus of the optic tract and the dorsal terminal nucleus of the wallaby, *Macropus eugenii*. *J Neurophysiol* 72:2927–2943
- Ilg UJ, Hoffmann KP (1993) Functional grouping of the corticopretectal projection. *J Neurophysiol* 70:867–869
- Karten HJ, Hodos W (1967) *A stereotaxic atlas of the brain of the pigeon (Columba livia)*. Johns Hopkins Press, Baltimore
- Karten HJ, Shimizu T (1989) The origins of the neocortex: connections and lamination as distinct events in evolution. *J Cogn Neurosci* 1:291–301
- Karten HJ, Fite KV, Brecha N (1977) Specific projection of displaced retinal ganglion cells upon the accessory optic system in the pigeon (*Columba livia*). *Proc Natl Acad Sci USA* 74:1752–1756
- Lent R (1982) The organization of subcortical projections of the hamster's visual cortex. *J Comp Neurol* 206:227–242
- Lui F, Giolli RA, Blanks RH, Tom EM (1994) Pattern of striate cortical projections to the pretectal complex in the guinea pig. *J Comp Neurol* 344:598–609
- McKenna OC, Wallman J (1985) Functional postnatal changes in avian brain regions responsive to retinal slip: a 2-deoxy-D-glucose study. *J Neurosci* 5:330–342
- Merabet L, Desautels A, Minville K, Casanova C (1998) Motion integration in a thalamic visual nucleus. *Nature* 396:265–268
- Miceli D, Giovanni H, Reperant J, Peyrichoux J (1979) The avian visual wulst. I. An anatomical study of afferent and efferent pathways. II. An electrophysiological study of the functional properties of single neurons. In: Granda, AM, Maxwell JH (eds) *Neural mechanisms of behavior of the pigeon*. Plenum Press, New York, pp 223–354
- Morgan B, Frost BJ (1981) Visual response properties of neurons in the nucleus of the basal optic root of pigeons. *Exp Brain Res* 42:184–188
- Movshon JA, Adelson EH, Gizzi MS, Newsome WT (1985) The analysis of visual moving patterns. In: Chagas C, Gattass R, Gross C (eds) *Study group on pattern recognition mechanisms*. Pontificia Academia Scientiarum, Vatican City, pp 117–151
- Mustari MJ, Fuchs AF, Kaneko CR, Robinson FR (1994) Anatomical connections of the primate pretectal nucleus of the optic tract. *J Comp Neurol* 349:111–128
- Papoulis A (1990) *Probability and statistics*. Prentice-Hall, New York
- Pereira A, Volchan E, Vargas CD, Penetra L, Rocha-Miranda CE (2000) Cortical and subcortical influences on the nucleus of the optic tract of the opossum. *Neuroscience* 95:953–963
- Reiner A, Brecha N, Karten HJ (1979) A specific projection of retinal displaced ganglion cells to the nucleus of the basal optic root in the chicken. *Neuroscience* 4:1679–88
- Rio JP, Villalobos J, Miceli D, Reperant J (1983) Efferent projections of the visual wulst upon the nucleus of the basal optic root in the pigeon. *Brain Res* 271:145–151
- Rodman HR, Albright TD (1989) Single-unit analysis of pattern-motion selective properties in the middle temporal visual area (MT). *Exp Brain Res* 75:53–64
- Scannell JW, Sengpiel F, Tovee MJ, Benson PJ, Blakemore C, Young MP (1996) Visual motion processing in the anterior ectosylvian sulcus of the cat. *J Neurophysiol* 76:895–907
- Schoppmann A (1981) Projections from areas 17 and 18 of the visual cortex to the nucleus of the optic tract. *Brain Res* 223:1–17
- Shintani T, Hoshino K, Meguro R, Kaiya T, Norita M (1999) A light and electron microscopic analysis of the convergent retinal and visual cortical projections to the nucleus of the optic tract (NOT) in the pigmented rat. *Neurobiology* 7:445–460
- Simpson JI (1984) The accessory optic system. *Annu Rev Neurosci* 7:13–41
- Simpson JI, Leonard CS, Soodak RE (1988) The accessory optic system. II. Spatial organization of direction selectivity. *J Neurophysiol* 60:2055–2072

- Smith AT, Harris LR (1991) Use plaid patterns to distinguish the cortical and direct retinal inputs to the brainstem optokinetic nystagmus generator. *Exp Brain Res* 86:324–332
- Stoner GR, Albright TD (1992) Neural correlates of perceptual motion coherence. *Nature* 358:412–414
- Stoner GR, Albright TD (1994) Visual motion integration. In: Smith TA, Snowden RJ (eds) *Visual detection of motion*. Academic Press, London, pp 253–290
- Welch L (1989) The perception of moving plaids reveals two motion-processing stages. *Nature* 337:734–736
- Wilson P (1980) The organization of the visual hyperstriatum in the domestic chick. II. Receptive field properties of single units. *Brain Res* 188:333–345
- Winterson BJ, Brauth SE (1985) Direction selective single units in the nucleus lentiformis mesencephali of the pigeon (*Columba livia*). *Exp Brain Res* 60:215–226
- Wolf-Oberhollenzer F, Kirschfeld K (1994) Motion sensitivity in the nucleus of the basal optic root of the pigeon. *J Neurophysiol* 71:1559–1573
- Wylie DR, Crowder NA (2000) Spatiotemporal properties of fast and slow neurons in the pretectal nucleus lentiformis mesencephali in pigeons. *J Neurophysiol* 84:2529–2540
- Wylie DR, Frost BJ (1990) Visual response properties of neurons in the nucleus of the basal optic root of the pigeon: a quantitative analysis. *Exp Brain Res* 82:327–336
- Wylie DR, Linkenhoker B, Lau KL (1997) Projections of the nucleus of the basal optic root in pigeons (*Columba livia*) revealed with biotinylated dextran amine. *J Comp Neurol* 384:517–536
- Zolotilina EG, Eremina SV, Orlov IV (1995) Horizontal optokinetic nystagmus in the pigeon during static tilts in the frontal plane. *Neurosci Behav Physiol* 25:300–306